Supplementary Information for

Graded Intrafillable Architecture-based Iontronic Pressure Sensor with Ultra-Broad-Range High Sensitivity

Ningning Bai,[1]† Liu Wang,[1,2]† Qi Wang,[1] Jue Deng,[1,2] Yan Wang,[1] Peng Lu,[1] Jun Huang,[1] Gang Li,[1] Yuan Zhang,[1] Junlong Yang,[1] Kewei Xie[1], Xuanhe Zhao[2], Chuan Fei Guo[1,3]*

[1]Department of Materials Science and Engineering and Centers for Mechanical Engineering Research and Education at MIT and SUSTech, Southern University of Science and Technology, Shenzhen 518055, China

[2]Department of Mechanical Engineering, Massachusetts Institute of Technology, Cambridge, MA 02139, USA.

[3]Shenzhen Engineering Research Center for Novel Electronic Information Materials and Devices, Southern University of Science and Technology, Shenzhen 518055, China

† Ningning Bai and Liu Wang contributed equally to this work.

*** Corresponding author. Email:** guocf@sustc.edu.cn

Supplementary Figures

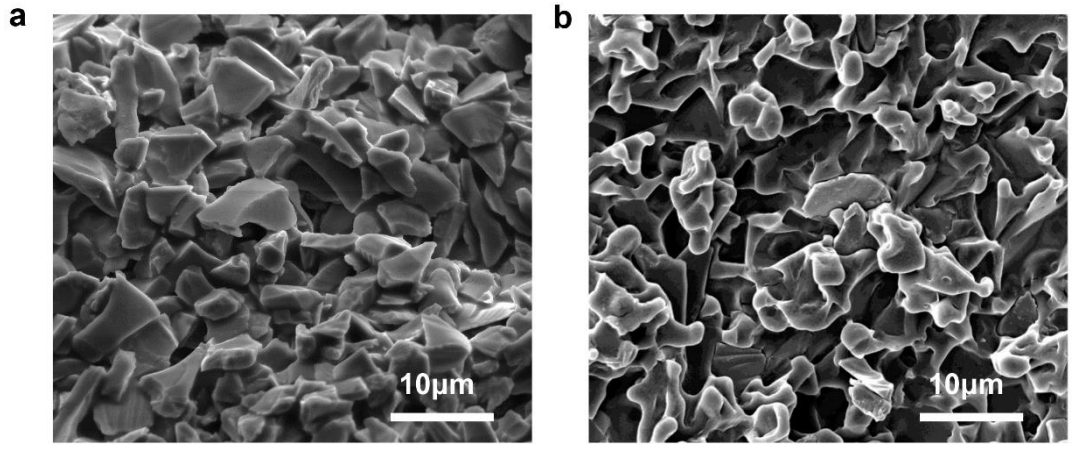

Supplementary Figure 1. SEM images. (a) Sandpaper template and **(b)** GIA film.

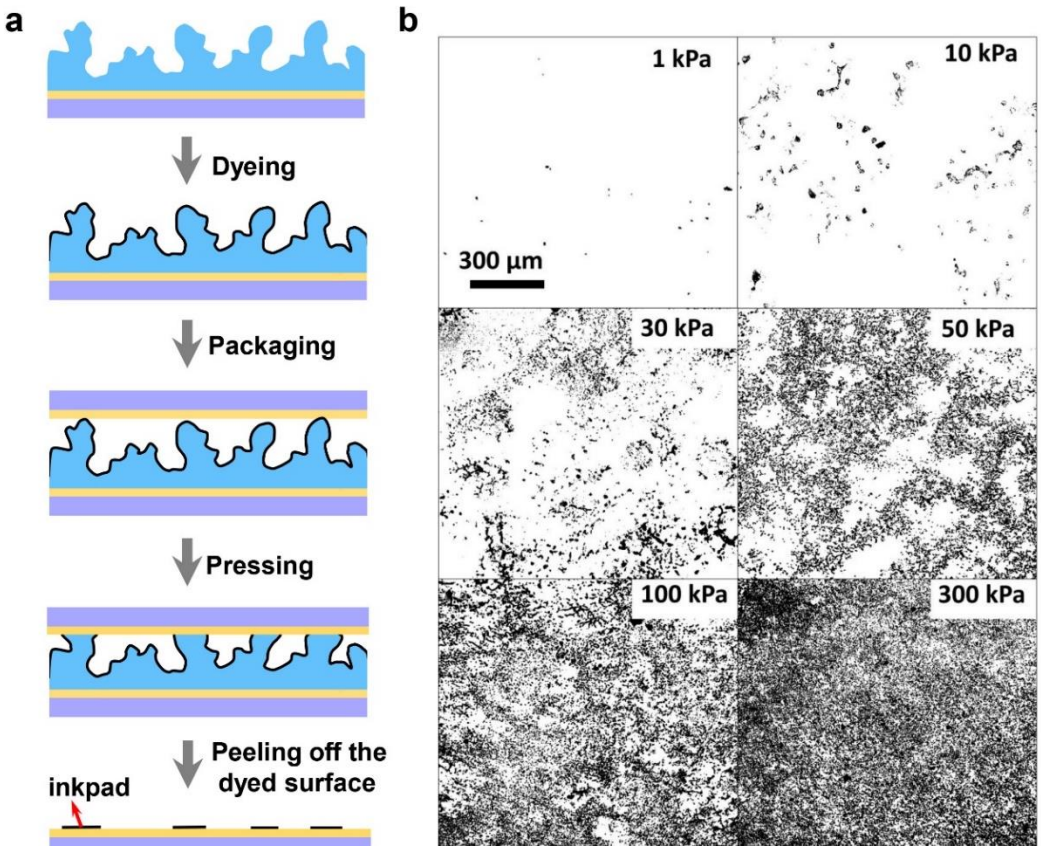

Supplementary Figure 2. Visualization of contact area between the PVA/H_3PO_4 GIA film and electrode under different pressures. (a) Diagram of dyeing of electrode upon loading. **(b)** Change of contact area between the PVA/H_3PO_4 GIA film and the electrode under different pressures.

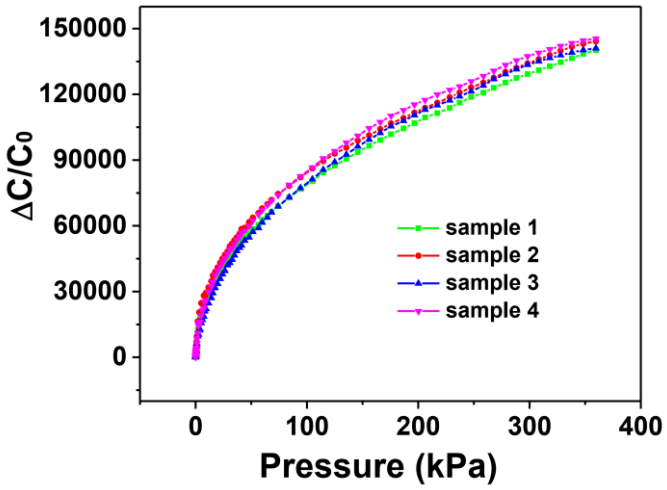

Supplementary Figure 3. Reproducibility test for capacitance change with the pressure of the GIA-based iontronic pressure sensors in different batches.

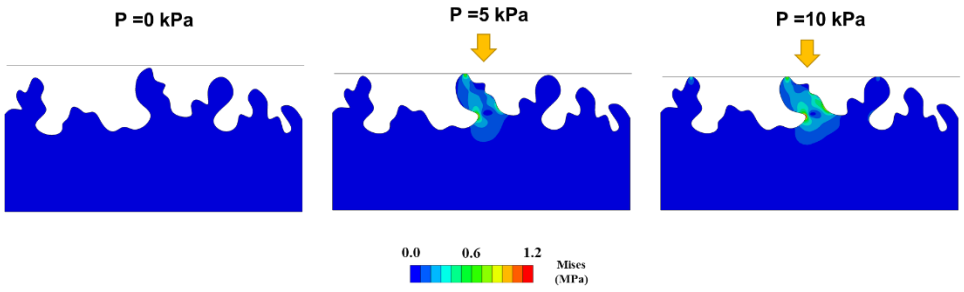

Supplementary Figure 4. Screen snapshots of finite element simulations at *P*=0, 5, 10 kPa.

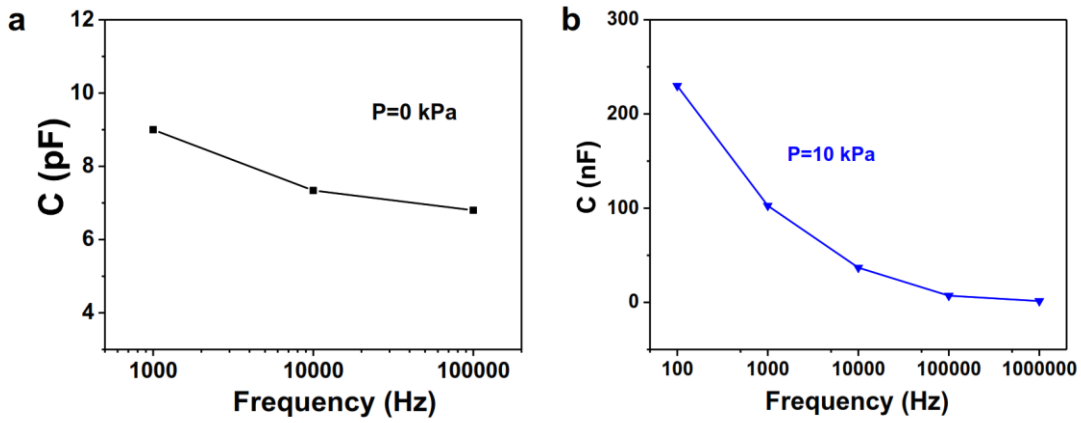

Supplementary Figure 5. Measured capacitance as a function of frequency. **(a)** Capacitance–frequency relation of GIA-based iontronic sensor before loading (P = 0 kPa). **(b)** Capacitance–frequency relation of GIA-based iontronic sensor under loading of 10 kPa.

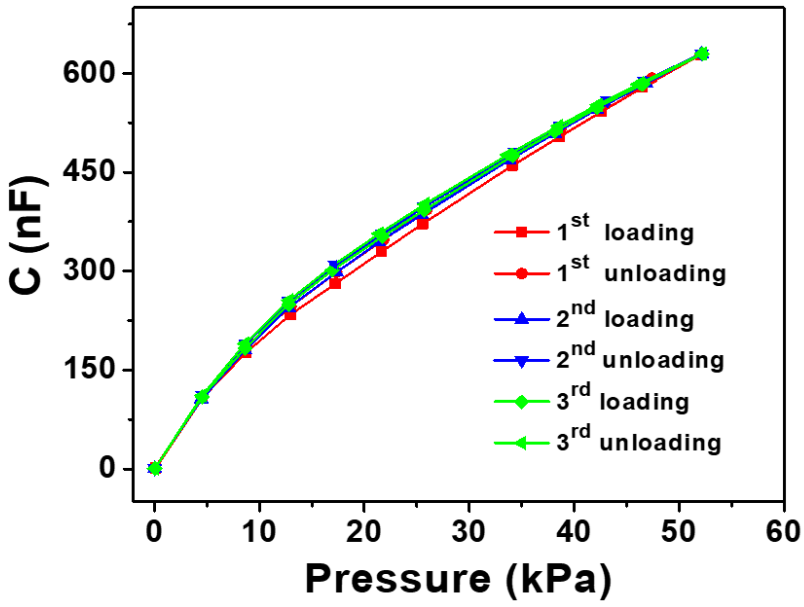

Supplementary Figure 6. Hysteresis of the iontronic pressure sensor under three loading (50 kPa)/unloading cycles.

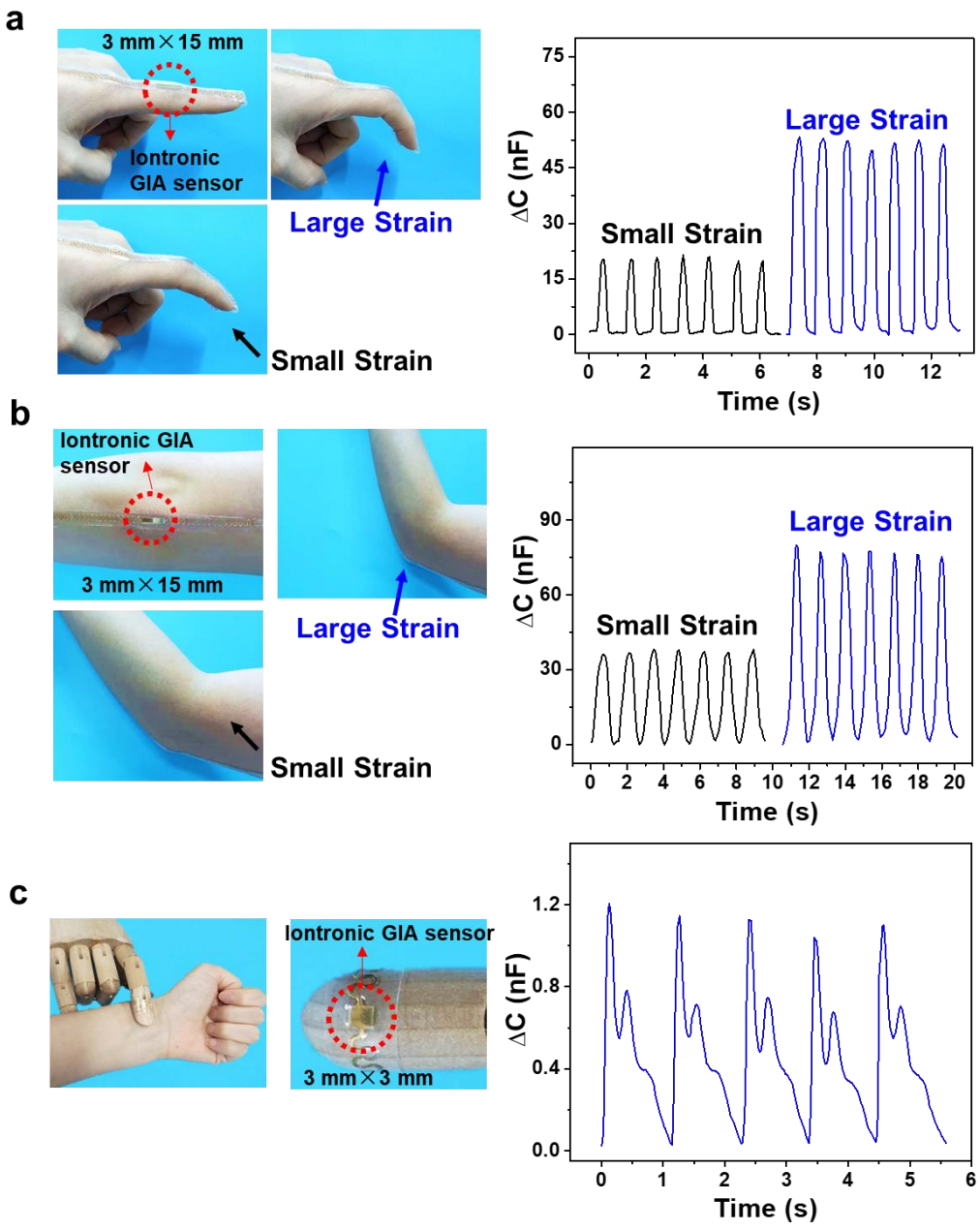

Supplementary Figure 7. Performance of GIA-based iontronic pressure sensor. Real-time monitoring of capacitance variations caused by repeated **(a)** forefinger bending and **(b)** elbow bending under different bending amplitude. **(c)** Pulse wave signals of the radial artery at the test frequency of 0.1 MHz.

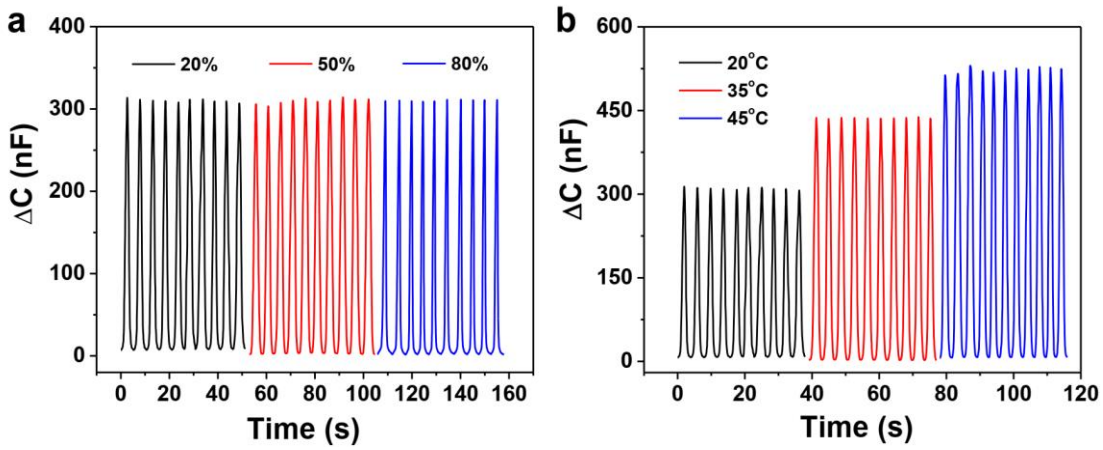

Supplementary Figure 8. Sensing performance under different conditions. (a) Relative humidity; **(b)** Temperatures.

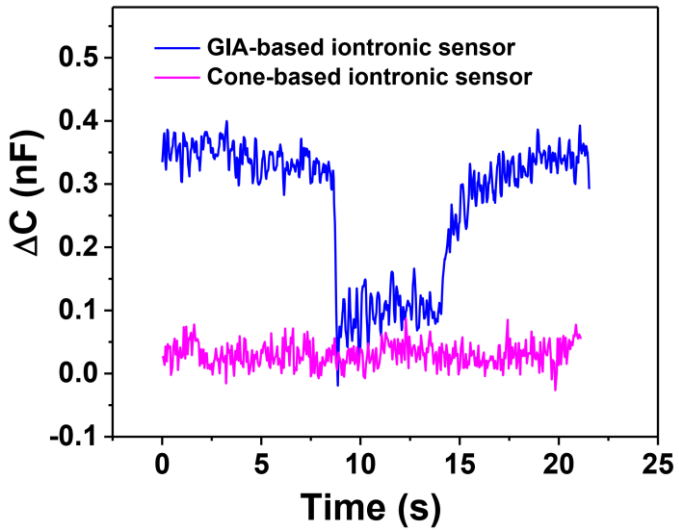

Supplementary Figure 9. Responses by unloading from/loading on a bag of paper towel (1.7 kg) to a car trunk using iontronic sensors applying GIA and with microcones, respectively.

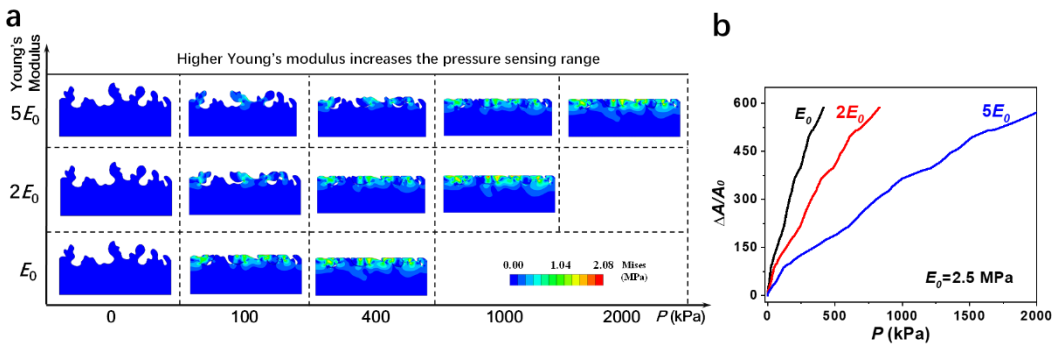

Supplementary Figure 10. Higher Young's modulus increases the pressure sensing range. (a) Finite element analyses of GIAs with different material moduli of $E_0, 2E_0$ and $5E_0$, where E_0 =2.5 MPa. When Young's modulus gets 5 times higher, the pressure sensing range can reach up to 2000 kPa. **(b)** Corresponding simulation results for normalized contact area as a function of applied pressure.

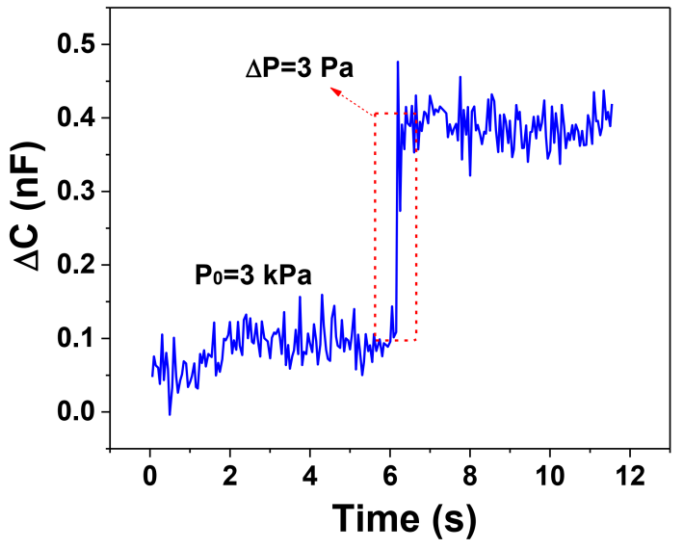

Supplementary Figure 11. Resolving a tiny pressure change of 3 Pa under a basic pressure of 3 kPa.

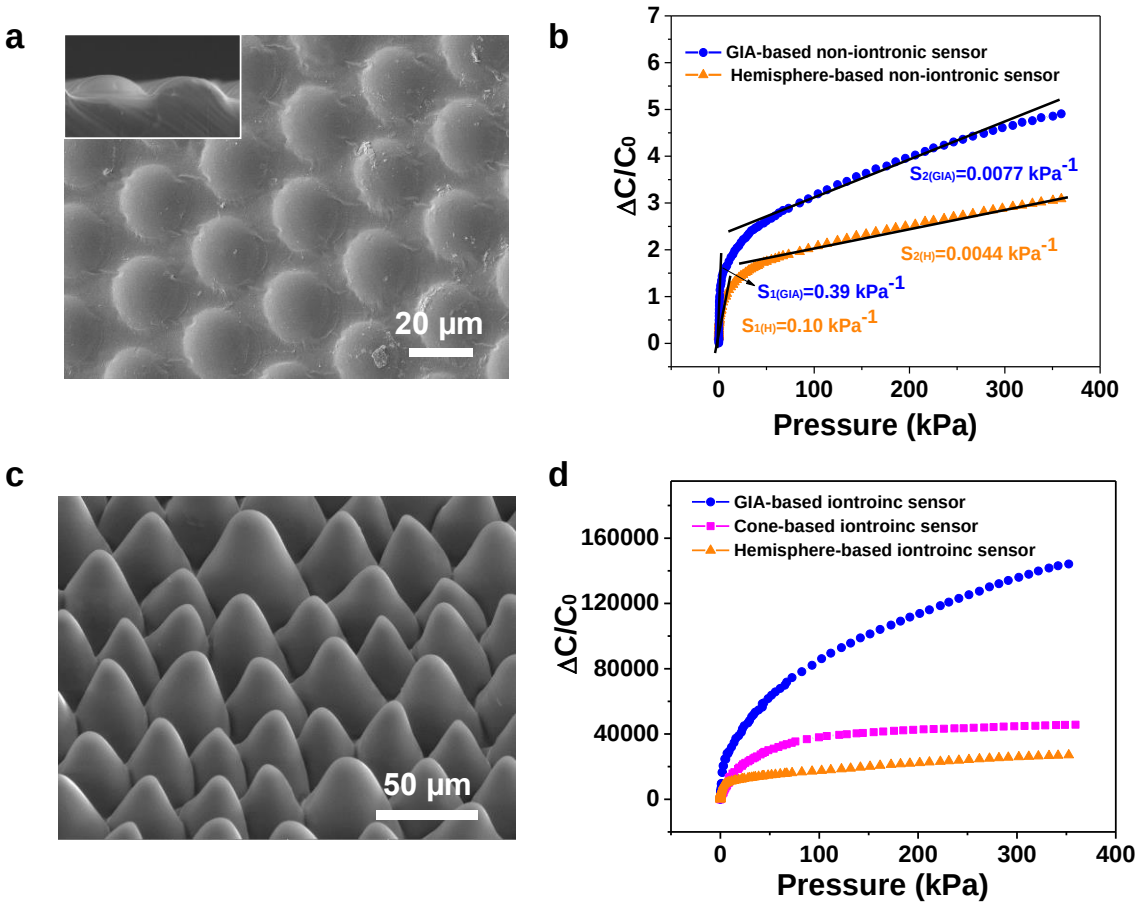

Supplementary Figure 12. Performance comparison among sensors applying the GIA, microstructured hemispheres and cones. (a) SEM image of the microstructured hemispheres. **(b)** Comparison of the change in capacitance with the pressure between GIA-based and hemisphere-based non-iontronic pressure sensors. **(c)** SEM image of the microstructured cones. **(d)** Comparison of the change in capacitance with increasing pressure among GIA-based, hemisphere-based, and cone-based iontronic pressure sensors.

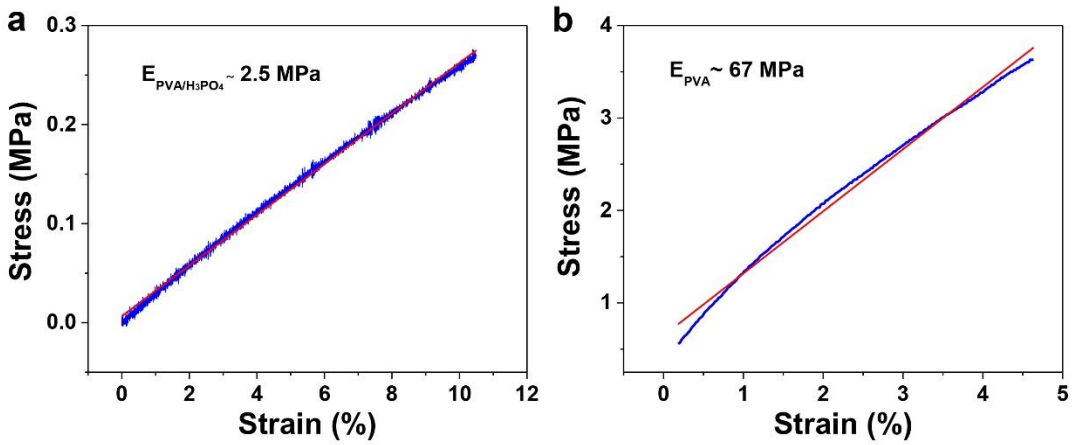

Supplementary Figure 13. Experimental stress-strain curves. **(a)** PVA/H_3PO_4 film and **(b)** PVA film. Blue lines are experimental data and red lines are fitted.

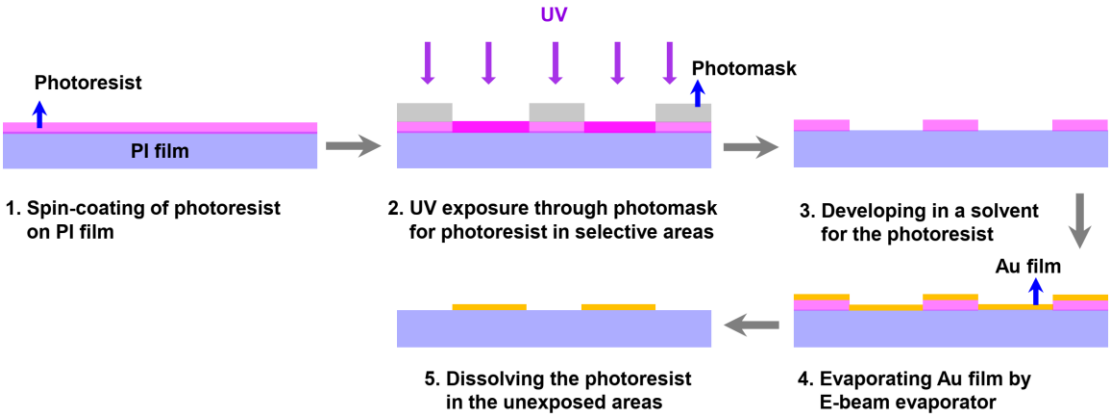

Supplementary Figure 14. Fabrication process of micro-electrodes.

Supplementary Tables

Supplementary Table 1. Capacitance density of GIA-based iontronic sensors with different device areas.

Device area (μm^2)	Capacitance density ($pF/\mu m^2$)
50 × 50	0.417
100 × 100	0.411
200 × 200	0.412